

## GRB-supernovae: A new spin on gravitational waves<sup>(\*)</sup>

M. H. P. M. VAN PUTTEN

*MIT-LIGO Project, NW 17-161, 175 Albany Street, Cambridge, MA 02139, USA*

(ricevuto il 23 Maggio 2005; pubblicato online il 3 Ottobre 2005)

**Summary.** — The discovery of the GRB-supernova association poses the question on the nature of the inner engine as the outcome of Type Ib/c supernovae. These events are believed to represent core-collapse of massive stars, probably in low-period stellar binaries and similar but not identical to the Type II event SN1987A. The branching ratio of Type Ib/c supernovae into GRB-supernovae has the remarkably small value of less than 0.5%. These observational constraints point towards a rapidly rotating black hole formed at low probability with low kick velocity. The putative black hole hereby remains centered, and matures into a high-mass object with large rotational energy in angular momentum. As the MeV-neutrino emissions from SN1987A demonstrate, the most powerful probe of the inner workings of core-collapse events are radiation channels to which the remnant envelope is optically thin. We here discuss the prospect of gravitational-wave emissions powered by a rapidly rotating central black hole which, in contrast to MeV-neutrinos, can be probed to distances as large as 100 Mpc through upcoming gravitational-wave detectors LIGO and Virgo. We identify the GRB-emissions, commonly attributed to ultrarelativistic baryon-poor ejecta, with a new process of linear acceleration of charged particles along the axis of rotation of a black hole in response to spin-orbit coupling. We include some preliminary numerical simulations on internal shocks produced by intermittent ejecta. The results showing a radial splash, which points towards low-luminosity and lower-energy radiation at large angles, possibly related to X-ray flashes.

PACS 98.70.Rz –  $\gamma$ -ray sources,  $\gamma$ -ray bursts.

PACS 01.30.Cc – Conference proceedings.

### 1. – Introduction

The Type Ib/c GRB-supernova association, beautifully demonstrated by GRB030329/SN2002dh, establishes SNIb/c as the parent population of cosmological gamma-ray bursts. This, in turn, confirms their association to massive stars proposed by Woosley [52,

---

<sup>(\*)</sup> Paper presented at the “4th Workshop on Gamma-Ray Burst in the Afterglow Era”, Rome, October 18-22, 2004.

19, 32]. Massive stars have characteristically short lifetimes, whereby GRB-supernovae track the cosmological event rate. This is quantitatively confirmed by agreement in their true-to-observed event rates of 450–500 based on two independent analysis, one on geometrical beaming factors and the other on locking to the cosmic star-formation rate [14, 45].

Furthermore, Type-II and Type-Ib/c supernovae are believed to represent the end-point of massive stars [13, 42] in binaries, such as in the Type-II/Ib event SN1993J [27]. This binary association suggests a hierarchy, wherein hydrogen-rich, envelope retaining SNII are associated with wide binaries, while hydrogen-poor, envelope stripped SNIb and SNIc are associated with increasingly compact binaries [29, 42]. By tidal coupling, the primary star in the latter will rotate at approximately the orbital period at the moment of core-collapse. With an evolved core [9], these events are therefore believed to produce a spinning black hole [52, 22, 8].

GRB-supernovae are rare, in view of the observed small branching ratio of less than 1% off their parent SNIb/c. While all SNIb/c may be producing black holes, only some are associated with the production of ultrarelativistic outflows powering gamma-ray emissions [36, 37]. Quite generally, black holes produced in core-collapse possess random kick velocities of a few hundred  $\text{km s}^{-1}$  [7]. Quite generally, therefore, black holes formed in core-collapse are parametrized by their mass  $M$ , angular momentum  $J$  and kick velocity  $K$ . By its kick velocity, a newly formed black hole typically escapes the central high-density regions of the progenitor star before core-collapse is completed. This suggests an association of GRB-supernovae with the small sample of black holes possessing low kick velocities [47]. In these cases, the black hole remains centered, surges into a high-mass object with a rotational energy of up to 66% of the maximal attainable value, and subsequently spins up by accretion or spins down in a suspended accretion state [47].

Spacetime around a rotating black hole is described by the Kerr metric [20]. It describes an exact solution of frame-dragging induced by the angular momentum of a black hole. Frame-dragging appears in nonzero angular velocities of zero angular momentum observers. Observational evidence for frame-dragging rotating black holes is successfully pursued through X-ray spectroscopy by ASCA and XMM in surrounding accretion disks [39, 18, 12]. Kerr black holes further possess an anomalously large energy reservoir in angular momentum. Per unit mass, this energy reservoir exceeds that of a rapidly spinning neutron star by at least an order of magnitude. Finally, this energy reservoir is entirely baryon-free.

Frame-dragging creates a large differential angular velocity between the black hole, when rapidly spinning, and surrounding matter. When the latter is unmagnetized, the black hole continues to accrete matter, enlarging it and spinning it up towards an extreme Kerr black hole along a Bardeen trajectory [4]. Alternatively, when the surrounding matter is uniformly magnetized, corresponding to two counter-oriented current rings [48], a spin-connection becomes effective between the angular momentum of the black hole and the inner regions of the surrounding accretion disk which forcefully spins down the black hole [47]. Especially at high spin rates, this process is facilitated by an equilibrium magnetic moment of the black hole in its lowest energy state. This process is self-sustaining, as most of the black-hole luminosity is incident onto the inner face of a surrounding torus, created with strong differential shear by competing torques acting on its inner and outer face. This energy input may be the agent driving a dynamo which creates superstrong magnetic fields. In a suspended accretion state, the large energy reservoir in black hole spin energy is released with an efficiency of  $\eta = \Omega_T/\Omega_H$  determined by the ratio of the angular velocity  $\Omega_T$  of the surrounding torus to the

angular velocity  $\Omega_H$  of the black hole. This energy release, on the order of  $10^{53}$  erg. This output is larger than that seen at present in the electromagnetic radiation of GRB-emissions and supernova ejecta (about  $10^{51}$  erg, corrected for beaming and asphericities). However, this additional energy output can be safely accounted for by “unseen” emissions in gravitational radiation and MeV-neutrino emissions [49, 48, 46].

Frame-dragging also acts along the axis of rotation. Here, it creates an energetic interaction along open magnetic flux-tubes (“ergo-tubes”) subtended by the event horizon of the black hole. These interactions define a new mechanism of accelerating magnetized ejecta to ultrarelativistic velocities. This spin-orbit coupling is a classical analogue of an earlier quantum mechanical treatment [44]. This application radically differs from the common view, that black-hole energetic processes are strictly confined to the action of frame-dragging in the ergosphere. We shall illustrate the case of intermittent ejecta with a numerical simulation, whose shocked interactions serve as input to baryon-poor outflows powering gamma-ray emissions [36, 37].

## 2. – Theoretical background

An extreme Kerr black hole reaches an angular velocity of its horizon given by  $\Omega_H = 1/2M$ . This angular velocity far surpasses that of surrounding matter, when separated from the event horizon by a distance on the order of the linear size of the black hole. According to the first law of thermodynamics, the efficiency of energy transfer from the black hole to the environment reaches a fraction

$$(1) \quad \eta = \frac{\Omega_T}{\Omega_H}$$

of its rotational energy  $E_{rot} = 2M \sin^2(\lambda/4)$ , where  $\sin \lambda$  the specific angular momentum of the black hole per unit mass and  $\Omega_T$  denotes the angular velocity of the surrounding torus. The torus itself is suspended by competing torques acting on its two faces, one positive torque on its inner face and a negative torque on its outer face due to generic losses in energy and angular momentum in magnetic winds. The question arises: what are the radiation channels through which the torus processes this input? We shall discuss this in the next section.

The Kerr metric shows black hole spin creating frame-dragging, described by particular contributions to the Riemann tensor [10]. In turn, the Riemann tensor couples to spin [30, 31, 35, 28]. Rotating black holes hereby couple to the angular momentum (and spin) of nearby particles. We note that the angular momentum per unit mass represents a rate of change of surface area, while the Riemann tensor has dimension  $\text{cm}^{-2}$  in geometrical units. Hence, curvature-spin coupling produces a force, whereby test particles follow non-geodesic trajectories [35]. These gravitational spin-angular momentum interactions are commonly referred to as gravitomagnetic effects [41] by analogy to magnetic moment-magnetic moment interactions, even though there is an interesting difference in sign. To quantify this in the application to outflows from black holes, we shall focus on spin-orbit interactions along the axis of rotation following [44]. Using dimensional analysis once more, the gravitational potential for spin aligned interactions should satisfy

$$(2) \quad E = \omega J,$$

where  $\omega$  refers to the frame-dragging angular velocity produced by the massive body and

$J$  is the angular momentum of the particle. Spinning bodies hereby couple to spinning bodies [21].

We shall detail the radiative process of (1) and (2) in case of a particular topology of the magnetosphere, consisting of a torus magnetosphere supported by two counter-oriented current rings and, formed by a change of topology from the outer layers of the inner torus magnetosphere, an open magnetic flux tube along the axis of rotation [49, 48].

### 3. – Radiation channels of a non-axisymmetric torus

The surrounding matter is strongly sheared by competing torques, which creates a torus with a super-Keplerian inner face and a sub-Keplerian outer face. For sufficiently strong viscosity —regulated by magnetohydrodynamical stresses— between the inner and the outer face, a state of suspended accretion can arise, in which the energy and angular momentum input from the black hole is balanced by energy and angular momentum losses to infinity. This *suspended accretion state* is described by balance equations of energy and momentum flux, and in many ways is equivalent to pulsars when viewed in poloidal topology [43, 48]. The kinetic energy of the torus intrudes a bound on the poloidal magnetic field-energy that it can support. We recently derived an estimate for the a maximal ratio of poloidal magnetic field energy-to-kinetic energy of the torus of about 1/12 [48].

Rapidly rotating black holes dissipate most of their spin-energy in the event horizon, set essentially by the spin-rate of the black hole. The lifetime of rapid spin hereby satisfies [48]

$$(3) \quad T_s \simeq 90 \text{ s} \left( \frac{M_H}{7M_\odot} \right) \left( \frac{\eta}{0.1} \right)^{-8/3} \left( \frac{\mu}{0.03} \right)^{-1}.$$

This estimate is consistent with durations of tens of seconds of long gamma-ray bursts.

The gravitational wave-emissions due to quadrupole emissions by a mass-inhomogeneity  $\delta M_T$  are [33]

$$(4) \quad L_{gw} = \frac{32}{5} (\omega \mathcal{M})^{10/3} F(e) \simeq \frac{32}{5} (M_H/R)^5 (\delta M_T/M_H)^2,$$

where  $\omega \simeq M^{1/2}/R^{3/2}$  denotes the orbital frequency of the torus with major radius  $R$ ,  $\mathcal{M} = (\delta M_T M_H)^{3/5}/(\delta M_T + M_H)^{1/5} \simeq M_H (\delta M_T/M_H)^{5/3}$  denotes the chirp mass, and  $F(e)$  denotes a geometric factor representing the ellipticity  $e$  of the orbital motion. The linearized result (4) has been amply confirmed by approximately one-solar luminosity in gravitational waves emitted by PSR1913+16 (with ellipticity  $e = 0.62$  [17, 40]). Here, we apply (4) to a non-axisymmetric torus around a black hole, whose mass-quadrupole inhomogeneity  $\delta M_T$  is determined self-consistently in a state of suspended accretion for the lifetime of rapid spin of the black hole. Quadrupole mass-moments will appear spontaneously due to non-axisymmetric waves whenever the torus is sufficiently slender.

The competing torques on the inner and outer face promote azimuthal shear in the torus, leading to a super-Keplerian state of the inner face and a sub-Keplerian state of the outer face. The torus becomes geometrically thick and may hereby become sufficiently slender to allow instability of quadrupole wave-modes  $m = 2$  for a minor-to-major radius less than 0.3260 [48]. This produces gravitational radiation at close to twice the angular frequency of the torus.

The equations of suspended accretion [48] can be solved algebraically, giving solutions for the total radiation energies emitted by the torus, expressed as fractions of the rotational energy of the black hole. Solving for the simultaneous output in gravitational radiation, MeV-neutrino emissions and magnetic winds, we find

$$(5) \quad E_{gw} \simeq 0.2M_{\odot} \left( \frac{\eta}{0.1} \right) \left( \frac{M_H}{7M_{\odot}} \right), \quad f_{gw} \simeq 500 \text{ Hz} \left( \frac{\eta}{0.1} \right) \left( \frac{7M_{\odot}}{M_H} \right)$$

in units of  $M_{\odot} = 2 \times 10^{54}$  erg. This appreciation (5) of GRBs typically surpasses the true energy  $E_{\gamma} \simeq 3 \times 10^{50}$  erg in gamma-rays [14] by several orders of magnitude with potentially some exceptions [15]. Sub-dominant emissions in magnetic winds power an accompanying supernova at a factor  $\eta$  less than that in gravitational radiation,

$$(6) \quad E_w = 4 \times 10^{52} \text{ erg} \left( \frac{\eta}{0.1} \right)^2 \left( \frac{M}{7M_{\odot}} \right).$$

The energy in torus winds (6) further provide a powerful agent towards various processes: an accompanying supernovae [8], possibly radiatively-driven and radio loud by dissipation of their magnetic energy [46], collimation of the enclosed baryon-poor outflows from the black hole [24], as well as a source of neutron pick-up by the same [25].

The energy output in thermal and MeV-neutrino emissions is a factor  $\delta$  less than that in gravitational radiation, or

$$(7) \quad E_{\nu} = 2 \times 10^{53} \text{ erg} \left( \frac{\eta}{0.1} \right) \left( \frac{\delta}{0.30} \right) \left( \frac{M_H}{7M_{\odot}} \right).$$

At this dissipation rate, the torus develops a temperature of a few MeV and produces baryon-rich winds [48].

#### 4. – Spin-orbit interactions $E = \Omega J$

A particle in a periodic orbit, *e.g.*, a charge particle in a Landau state confined to a surface of constant magnetic flux, carries orbital angular momentum. Geometrically, this motion represents a rate of change of surface area an associated spacelike two-surface, following the dimensional analysis mentioned in the previous section. This two-surface can be identified by considering the helical motion as seen in four-dimensional spacetime [50]. The result is an interaction with the Riemann tensor—the Papapetrou interaction between spin or angular momentum with curvature [30,31].

The Kerr metric embodies an exact solution to spin-induced curvature, expressed by the appearance of frame-dragging in the Riemann-curvature. Not surprisingly, the Papapetrou spin-curvature coupling produces spin-coupling to the frame-dragging angular velocity. In a neighborhood of the axis of rotational of the black hole, this gives rise to (2). To see this, we may use the non-zero components of the Riemann tensor of the Kerr metric in Boyer-Lindquist coordinates relative to tetrad 1-forms given by Chandrasekhar [10]. Accordingly, the Riemann tensor creates the radial force [50]

$$(8) \quad F_2 = JR_{3120} = JAD = -\partial_2 \omega J.$$

The assertion (2) follows from

$$(9) \quad E = \int_r^\infty F_2 ds = \omega J.$$

The result (9) also follows from a completely independent derivation, by considering the difference in total energy between two particles in counter rotating orbits about the axis of rotation of the black hole. We insist that these two particles have angular momenta of opposite sign and equal magnitude,  $J_\pm = g_{\phi\phi} u^t (\Omega_\pm - \omega)$ , where  $u^b$  denotes their velocity four-vectors. Thus, we have

$$(10) \quad J_\pm = g_{\phi\phi} u^t \sqrt{\omega^2 - (g_{tt} + (u^t)^{-2})/g_{\phi\phi}} = \pm J.$$

This shows that  $u^t$  is the same for each particle. The total energy of the particles is given by  $E_\pm = (u^t)^{-1} + \Omega_\pm J_\pm$ , and hence one-half their difference [50]

$$(11) \quad E = \frac{1}{2}(E_+ - E_-) = \omega J.$$

A perfectly conducting blob of charged particles in a magnetic field in electrostatic equilibrium is characterized by rigid rotation [41] with angular velocity  $\Omega_b$ . In the frame of zero angular momentum observers, the local charge-density is given by the Goldreich-Julian charge density [16]. In the lowest energy state with vanishing canonical angular momentum, the angular momentum of the charge particles satisfies  $J = eA_\phi$ , where  $e$  denotes the unit of electric charge and  $A_\phi$  the  $\phi$ -component of the electromagnetic vector potential  $A_a$  [44].

Consider blob of charged particles in an open magnetic flux tube about the axis of rotation of the black hole with magnetic flux  $2\pi A_\phi$ . The number  $N(s)$  of particles per unit height  $s$  of the blob, therefore, satisfies  $N(s) = (\Omega_b - \omega)A_\phi/e$ , where  $e$  denotes the elementary charge. A pair of blobs in both directions along the spin-axis of scale height  $h$  hereby receives an energy

$$(12) \quad E_{blob} = \omega J N h = \omega(\Omega_b - \omega)A_\phi^2 h = (1 \times 10^{47} \text{ erg}) B_{15} h_M^3 H,$$

where  $h_M = h/M$  denotes the linear dimension of the blob,  $B_{15} = B/10^{15}$ . Here, we use the normalized function  $H = 4\hat{\omega}(\hat{\Omega}_b - \hat{\omega})$ , where  $\hat{\omega} = \omega/\Omega_H$  and  $\hat{\Omega}_b = \Omega_b/\Omega_H$ . Charged particles in superstrong magnetic fields are essentially massless. The ejection of a pair of blobs with energy (12) hereby takes place in a light-crossing time of about 0.3 ms for a stellar mass black hole, such as a seven solar mass black hole of linear dimension  $10^7$  cm. This corresponds to an instantaneous luminosity on the order of  $3 \times 10^{50}$  erg/s.

An intermittent source produces iterated emissions of blobs —“pancakes” in the observer’s frame [34]— which can dissipate their kinetic energy in collisions in the internal shock model of gamma-ray bursts [36, 37]. Figure 1 shows a relativistic simulation of such internal shock using JETLAB F90.

This presentation in terms of blobs is complementary to discussions on continuous outflows [26], wherein gamma-ray emissions are attributed to shocks due to by steepening by temporal fluctuations or intermittency at the source [23], or late-time interaction with the environment.

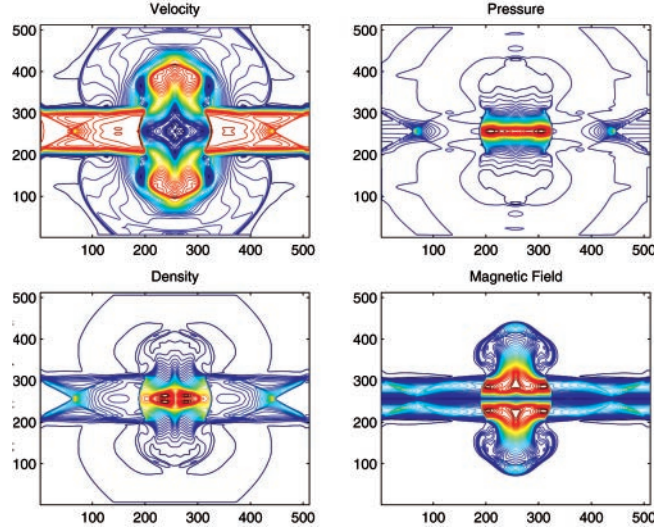


Fig. 1. – The head-on two magnetized ejecta (“kissing jets”) in the comoving frame of the center of mass, representing the collision of a fast blob overtaking a slow blob at large distances from an intermittent source. The simulation by JETLAB F90 has incoming flows each with Lorentz factor 1.5, and densities a few times that of the unmagnetized environment. A high-energy density region forms about a comoving stagnation point with strong amplification of the transverse magnetic field, and a radial splash produced by a pressure-driven, subsonic and radially outgoing flow with accompanying cocoon. This transverse morphology points towards accompanying low-luminosity low-energy gamma-ray or X-ray emissions over large angles.

## 5. – GRB-supernovae as long-duration burst sources for LIGO/Virgo

The predicted gravitational radiation (5) is in the range of sensitivity of the broad band detectors LIGO [1, 5] and Virgo [6, 2, 38] shown in fig. 2, as well as GEO [11, 51] and TAMA [3]. Matched filtering gives a theoretical upper bound on the signal-to-noise ratio in the detection of the long bursts in gravitational radiation from GRB-supernovae, shown in fig. 2. As a hydrodynamical source, the frequency will be unsteady at least on an intermittent timescales, so that a time-frequency trajectory method is probably more applicable in practice [46]. The signal-to-noise ratio will hereby be between first- and second-order detection algorithms.

As the outcome of Type-Ib/c supernovae, GRB-SNe are an astrophysical source population locked to the cosmic star-formation rate. Thus, their contribution to the stochastic background in gravitational radiation can be estimated semi-analytically, given the band-limited signals assuming  $B = \Delta f/f_e$  of around 10%, where  $f_e$  denotes the average gravitational-wave frequency in the comoving frame. Here, we can use the scaling relations  $E_{gw} = E_0 M_H/M_0$ ,  $f_e = f_0 M_0/M_H$ , where  $M_0 = 7M_\odot$ ,  $E_0 = 0.203M_\odot\eta_{0.1}$  and  $f_0 = 455\text{Hz}\eta_{0.1}$ , assuming maximal spin-rates ( $E_{rot} = E_{rot, max}$ ). For non-extremal black holes, a commensurate reduction factor in energy output can be inserted.

Assuming a uniform distribution of black hole masses, *e.g.*,  $M_H = (4 - 14) \times M_\odot$ , uncorrelated to the relative angular velocities  $\eta$  of the torus, summation gives an expected

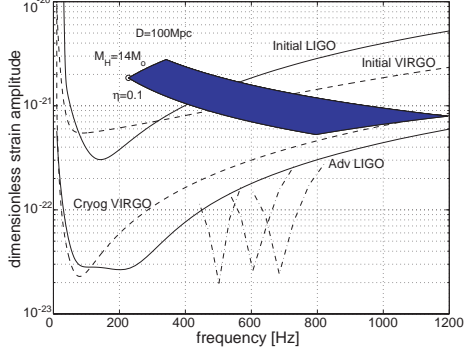


Fig.2

Fig. 2. – The expected distribution of strain amplitudes of GRB-supernovae and the design targets for the strain noise amplitude of the LIGO and Virgo detectors in the  $h(f)$ -diagram. The fiducial source distance is 100 Mpc, corresponding event rate is about one per year.

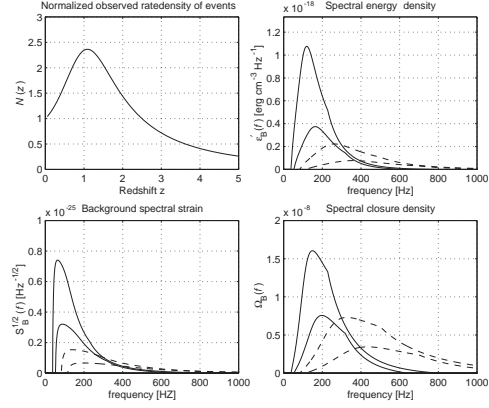


Fig.3

Fig. 3. – The expected cosmological distribution of GRB-supernovae to the stochastic background in gravitational radiation, on the basis of their correlation to the cosmic star-formation rate  $N(z)$ . (Reprinted from [50]©Cambridge University Press.)

spectral energy-density [46]

$$(13) \quad \langle \epsilon'_B(f) \rangle = 1.08 \times 10^{-18} \hat{f}_B(x) \text{ erg cm}^{-3} \text{ Hz}^{-1},$$

where  $\hat{f}_B(x) = f_B(x)/\max f_B(\cdot)$  is a normalized frequency distribution. The associated dimensionless amplitude  $\sqrt{S_B(f)} = \sqrt{2G/\pi c^3} f^{-1} \tilde{F}_B^{1/2}(f)$ , where  $\tilde{F}_B = c\epsilon'_B$  and  $G$  denotes Newton's constant, satisfies

$$(14) \quad \sqrt{S_B(f)} = 7.41 \times 10^{-26} \eta_{0.1}^{-1} \hat{f}_S^{1/2}(x) \text{ Hz}^{-1/2}$$

where  $\hat{f}_S(x) = f_S(x)/\max f_S(\cdot)$ ,  $f_S(x) = f_B(x)/x^2$ . Likewise, we have for the spectral closure density  $\Omega_B(f) = f\tilde{F}_B(f)/\rho_c c^3$  relative to the closure density  $\rho_c = 3H_0^2/8\pi G$

$$(15) \quad \tilde{\Omega}_B(f) = 1.60 \times 10^{-8} \eta_{0.1} \hat{f}_\Omega(x),$$

where  $\hat{f}_\Omega(x) = f_\Omega(x)/\max f_\Omega(\cdot)$ ,  $f_\Omega(x) = x f_B(x)$  and  $H_0$  denotes the Hubble constant.

The results are shown in Figs. (2-3). The extremal value of  $\Omega_B(f)$  is in the neighborhood of the location of maximal sensitivity of LIGO and Virgo.

\* \* \*

The author thanks A. LEVINSON, E. SCHURYAK, R. PREECE, A. LEVINSON, R. P. KERR for their constructive comments. This research is supported by the LIGO Observatories, constructed by Caltech and MIT with funding from NSF under cooperative agreement PHY 9210038. The LIGO Laboratory operates under cooperative agreement PHY-0107417.



## REFERENCES

- [1] ABRAMOVICI A., ALTHOUSE W. E., DREVER R. W. P. *et al.*, *Science*, **292** (1992) 325.
- [2] ACERNESE F. *et al.*, *Class. Quant. Grav.*, **19** (2002) 1421.
- [3] ANDO M. and the TAMA Collaboration, *Class. Quant. Grav.*, **19** (2001) 1409.
- [4] BARDEEN J. M., PRESS W. H., and TEUKOLSKY S. A., *ApJ*, **178** (1972) 347.
- [5] BARISH B., and WEISS R., *Phys. Today*, **52** (1999) 44.
- [6] BRADASCHIA C., DEL FABBRO R., DI VIRGILIO A. *et al.*, *Phys. Lett. A*, **163** (1992) 15.
- [7] BEKENSTEIN J. D., *ApJ*, **183** (1973) 657.
- [8] BETHE H. A., BROWN G. E. and LEE C.-H., *Selected Papers: Formation and Evolution of Black Holes in the Galaxy* (World Scientific, 2003).
- [9] BROWN G. E., LEE C.-H., WIJERS R. A. M. J., LEE H. K., ISRAELIAN G. and BETHE H. A., *NewA*, **5** (2000) 191.
- [10] CHANDRASEKHAR S., *The Mathematical Theory of Black Holes* (University Press, Oxford) 1983.
- [11] DANZMANN K., in *First Edoardo Amaldi Conf. Grav. Wave Experiments*, edited by E. COCCIA, G. PIZELLA and F. RONGA (World Scientific, Singapore) 1995, p. 100.
- [12] FABIAN A. C., *From X-ray Binaries to Quasars: Black Hole Accretion on All Mass Scales*, edited by T. J. MACCARONE, R. P. FENDER and L. C. HO (Kluwer, Dordrecht) 2004.
- [13] FILIPENKO A. V., *ARA&A*, **35** (1997) 309.
- [14] FRAIL D. A., KULKARNI S. R., SARI R. *et al.*, *ApJ*, **562** (2001) L55.
- [15] GHIRLANDA *et al.*, *ApJ*, **616** (2004) 331.
- [16] GOLDBREICH P., and JULIAN W. H., *ApJ*, **157** (1969) 869.
- [17] HULSE R. A. and TAYLOR J. H., *ApJ*, **1975** (195) L51.
- [18] IWASAWA K., FABIAN A. C., REYNOLDS C. S. *et al.*, *MNRAS*, **282** (1996) 1038.
- [19] KATZ J. I., *ApJ*, **432** (1994) L27.
- [20] KERR R. P., *Phys. Rev. Lett.*, **11** (1963) 237.
- [21] O'CONNEL R. F., *Phys. Rev. D.*, **10** (1974) 3035.
- [22] LEE C.-H., BROWN G. E. and WIJERS R. A. M. J., *ApJ*, **575** (2002) 996.
- [23] LEVINSON A., VAN PUTTEN M. H. P. M., *ApJ*, **488** (1977) 69.
- [24] LEVINSON A., and EICHLER D., *Phys. Rev. Lett.*, **2000** (85) 236.
- [25] LEVINSON A., and EICHLER D., *ApJ*, **594** (2003) L19.
- [26] LEVINSON A., *ApJ*, **608** (2004) 411.
- [27] MAUND J. R., SMARTT S. J., KUDRITZKI R. P., PODSIADOWSKI P. and GILMORE G. F., *Nature*, **427** (2004) 129.
- [28] MISNER, THORNE K. S. and WHEELER A., *Gravitation* (Freeman, San Francisco) 1974.
- [29] NOMOTO K., IWAMOTO K. and SUZUKI T., *Phys. Rep.*, **256** (1995) 173.
- [30] PAPAPETROU A., *Proc. Roy. Soc.*, **209** (1951) 248.
- [31] PAPAPETROU A., *Proc. Roy. Soc.*, **209** (1951) 259.
- [32] PACZYŃSKI B. P., *ApJ*, **494** (1998) L45.
- [33] PETERS P. C. and MATHEWS J., *Phys. Rev.*, **131** (1963) 435.
- [34] PIRAN T., astro-ph/0405503 (2004).
- [35] PIRANI F. A. E., *Act. Phys. Pol.*, **XV** (1956) 389.
- [36] REES M. J. and MÉSZÁROS P., *MNRAS*, **258** (1992) 41P.
- [37] REES M. J. and MÉSZÁROS P., *ApJ*, **430** (1994) L93.
- [38] SPALLICI A. D. A. M., AOUDIA S., DE FREITAS PACHECO J. A. *et al.*, gr-qc archive (2004) gr-qc/0406076.
- [39] TANAKA Y., NANDRA K. and FABIAN A.C., *Nature*, **375** (1995) 659.
- [40] TAYLOR J. H., *Rev. Mod. Phys.*, **66** (1994) 711.
- [41] THORNE K. S., PRICE R. H. and MACDONALD D. A., *Black Holes: The Membrane Paradigm* (Yale University Press, New Haven) 1986.
- [42] TURATTO M., *Supernovae and Gamma-ray Bursters*, edited by K.W. WEILER (Springer-Verlag, Heidelberg) 2003, p. 21.
- [43] VAN PUTTEN M. H. P. M., *Science*, **284** (1999) 115.
- [44] VAN PUTTEN M. H. P. M., *Phys. Rev. Lett.*, **84** (2000) 3752.

- [45] VAN PUTTEN M. H. P. M. and REGIMBAU T., *ApJ*, **593** (2003) L15.
- [46] VAN PUTTEN M. H. P. M., LEVINSON A., LEE H.-K., REGIMBAU T. and HARRY G., *Phys. Rev. D.*, **69** (2004) 044007.
- [47] VAN PUTTEN M. H. P. M., *ApJ*, **611** (2004) L81.
- [48] VAN PUTTEN M. H. P. M. and LEVINSON A., *ApJ*, **584** (2003) 953.
- [49] VAN PUTTEN M. H. P. M., *Phys. Rev. Lett.*, **87** (2001) 091101.
- [50] VAN PUTTEN M. H. P. M., *Gravitational Radiation, Luminous Black Holes and Gamma-ray Burst Supernovae* (Cambridge: Cambridge University Press) 2005.
- [51] WILLKE B. *et al.*, *Class. Quant. Grav.*, **19** (2002) 1377.
- [52] WOOSLEY S. E., *ApJ*, **405** (1993) 273.